

Original Research



Synergistic anti-tumor efficacy of mutant isocitrate dehydrogenase 1 inhibitor SYC-435 with standard therapy in patient-derived xenograft mouse models of glioma

Mari Kogiso^{a,b}, Lin Qi^{a,b,c}, Yuchen Du^{a,b,c}, Frank K. Braun^{a,b}, Huiyuan Zhang^{a,b}, L. Frank Huang^d, Lei Guo^e, Yulun Huang^{a,b,f}, Wan-Yee Teo^{b,g}, Holly Lindsay^{a,b}, Sibao Zhao^{a,b}, Sarah G. Injac^{a,b}, Zhen Liu^h, Vidya Mehta^{b,i}, Diep Tran^{b,i}, Feng Li^j, Patricia A. Baxter^b, Jack M. Su^b, Laszlo Perlaky^b, D. Williams Parsons^b, Murali Chintagumpala^b, Adekunle Adesina^{b,i}, Yongcheng Song^h, Xiao-Nan Li^{a,b,c,*}

^a Laboratory of Molecular Neuro-Oncology, Department of Pediatrics, Preclinical Neuro-Oncology Research Program, Baylor College of Medicine, Houston, TX 77030, USA

^b Texas Children's Cancer Center, Texas Children's Hospital, Houston, TX 77030, USA

^c Department of Pediatrics, Program of Precision Medicine PDOX Modeling of Pediatric Tumors, Simpson Querrey Biomedical Research Center, Ann & Robert H. Lurie Children's Hospital of Chicago, Northwestern University Feinberg School of Medicine, Chicago, IL 60611, USA

^d Division of Experimental Hematology and Cancer Biology, Brain Tumor Center, Cincinnati Children's Hospital Medical Center, Department of Pediatrics, University of Cincinnati College of Medicine, Cincinnati, OH 45229, USA

^e Texas A&M Health Science Center, Institute of Biosciences and Technology, Houston, TX 77030, USA

^f Department of Neurosurgery, Brain and Nerve Research Laboratory, the First Affiliated Hospital, Soochow University Medical School, Suzhou, Jiangsu 215007, China

^g Cancer and Stem Cell Biology Program, Duke-NUS Medical School, National Cancer Center, KK Women's and Children's Hospital, Humphrey Oei Institute of Cancer Research, Institute of Molecular and Cell Biology, A*STAR, 169610, Singapore

^h Department of Pharmacology, Baylor College of Medicine, Houston, TX 77030, USA

ⁱ Department of Pathology, Baylor College of Medicine, Houston, TX 77030, USA

^j Department of Pathology, Alkek Center for Drug Discovery, Advanced Technology Core, Baylor College of Medicine, Houston, TX 77030, USA

ARTICLE INFO

Keywords:

IDH1
SYC-435
Glioma
Standard therapy
Orthotopic PDX

ABSTRACT

Clinical outcomes in patients with WHO grade II/III astrocytoma, oligodendroglioma or secondary glioblastoma remain poor. Isocitrate dehydrogenase 1 (IDH1) is mutated in > 70% of these tumors, making it an attractive therapeutic target. To determine the efficacy of our newly developed mutant IDH1 inhibitor, SYC-435 (1-hydroxypyridin-2-one), we treated orthotopic glioma xenograft model (IC-BT142AOA) carrying R132H mutation and our newly established orthotopic patient-derived xenograft (PDX) model of recurrent anaplastic oligoastrocytoma (IC-V0914AOA) bearing R132C mutation. In addition to suppressing IDH1 mutant cell proliferation *in vitro*, SYC-435 (15 mg/kg, daily x 28 days) synergistically prolonged animal survival times with standard therapies (Temozolomide + fractionated radiation) mediated by reduction of H3K4/H3K9 methylation and expression of mitochondrial DNA (mtDNA)-encoded molecules. Furthermore, RNA-seq of the remnant tumors identified genes (*MYO1F*, *CTCI* and *BCL9*) and pathways (base excision repair, TCA cycle II, sirtuin signaling, protein kinase A, eukaryotic initiation factor 2 and α -adrenergic signaling) as mediators of therapy resistance. Our data demonstrated the efficacy SYC-435 in targeting IDH1 mutant gliomas when combined with standard therapy and identified a novel set of genes that should be prioritized for future studies to overcome SYC-435 resistance.

* Corresponding author: Xiao-Nan Li, M.D., Ph.D., Program of Precision Medicine PDOX Modeling of Pediatric Tumors, Ann & Robert H. Lurie Children's Hospital of Chicago; Department of Pediatrics, Northwestern University Feinberg School of Medicine, Simpson Querrey Biomedical Research Center, 4th floor, Room 4-522, 303 E. Superior St, Chicago, IL 60611; Phone: 312-503-6396.

E-mail address: XLi@luriechildrens.org (X.-N. Li).

<https://doi.org/10.1016/j.tranon.2022.101368>

Received 18 December 2021; Received in revised form 23 January 2022; Accepted 8 February 2022

1936-5233/© 2022 Published by Elsevier Inc. This is an open access article under the CC BY-NC-ND license (<http://creativecommons.org/licenses/by-nc-nd/4.0/>).

Introduction

Isocitrate dehydrogenase (IDH) is one of the key enzymes in the tricarboxylic acid cycle for aerobic metabolism of carbohydrates and fats. IDH catalyzes oxidative decarboxylation of isocitric acid to produce α -ketoglutaric acid (α -KG). There are three IDH isozymes in humans, with IDH1 located in cytoplasm and IDH2 and 3 in mitochondria [1,2]. Mutant IDH enzymes mostly lose the function of wild-type (WT) enzyme. However, the mutant enzyme catalyze the NADPH-dependent reduction of α -KG to R(-)-2-hydroxyglutarate (2-HG) leading to accumulation of 2-HG [3]. 2-HG is an inhibitor of α -KG dependent histone demethylases as well as DNA methyl hydroxylases [4] causing a genome-wide histone/DNA hypermethylation phenotype and cancer initiation.

IDH1 mutation occurs in > 70% of WHO grades II/III astrocytomas and oligodendrogliomas and secondary glioblastoma (GBM) [5]. The majority of mutations in the IDH1 gene in gliomas are R132H (91.5–92.3%), with R132C (3.7–4.3%) the second most common mutation type [6,7]. Genomic analysis showed that mutations in IDH1 preferentially occurred in younger patients with GBM and mutations in IDH1 were found in nearly all of the patients with secondary GBMs [8]. IDH1 mutations are very early events in gliomagenesis [9]. To date, IDH1 mutation has been recognized as a decisive genetic signpost of secondary GBM [10]. Therefore, this mutation could be a distinctive target for the treatment of secondary GBM. Indeed, treatment with a selective IDH1-R132H inhibitor (AGI-5198) suppressed tumor volume [11] and mutant IDH1 inhibitor MRK-A combination with CYP450 inhibitor aminobenzotriazole (ABT) significantly prolonged animal survival [12] in R132H-IDH1 mutant xenograft mouse models. While suppressive effects on tumor growth by inhibition of mutant IDH1 has been reported, patients with IDH1 mutations have significantly improved prognoses compared to patients with WT IDH1 [5]. Therefore, the clinical significance of mutant IDH1 inhibition is controversial.

1-hydroxypyridin-2-one named SYC-435 is a novel investigational mutant IDH1 inhibitor [13]. Similar to other mutant IDH1 inhibitors [11,14], SYC-435 is a potent inhibitor of not only R132H mutants but also R132C-IDH1 mutants [13]. SYC-435 has a smaller molecular weight (MW) of 215.3 than existing mutant IDH1 inhibitors, such as AGI-5198 (MW: 462.56) and AG-120 (MW: 582.96) [14]. This smaller MW may give SYC-435 a higher chance to cross the blood-brain barrier (BBB) and enter intracranial tumors.

The current standard therapy for newly diagnosed GBM is maximal surgical resection, followed by radiation with concurrent and adjuvant chemotherapy with temozolomide (TMZ). With these therapies, the median survival was 14.6 months and the two-year survival rate was 26.5% [15]. Therapeutic efficacy of standard therapy is still poor. Many glioma patients have been treated or will be treated with standard therapy. Therefore, testing synergistic effects of SYC-435 with standard therapy in pre-clinical animal models of GBM is an area of interest.

To establish the pre-clinical rationale for treatment with the mutant IDH1 inhibitor including SYC-435, animal models with this mutation are needed. Currently, pre-clinical animal models of high grade glioma with mutant IDH1 are limited to BT142 [16], TS603 [11] and GB10 [12], all of which harbor the R132H mutation. In this study, we established and characterized a new orthotopic patient-derived xenograft (PDX) mouse model of recurrent anaplastic oligoastrocytoma (AOA) (IC-V0914AOA) with an IDH1-R132C mutation. Using this model and BT142AOA, we examined the therapeutic efficacy of the mutant IDH1 inhibitor SYC-435 alone and in combination with standard therapy to establish pre-clinical rationale.

Materials and methods

Glioma models and tissue samples

An established neurosphere line of BT142 mut/- anaplastic

oligoastrocytoma (AOA) (WHO grade III) [16] (catalog#ACS-1018) was obtained from American Type Culture Collection (Manassas, VA). Patient tumor of V0914 recurrent AOA (WHO grade III) and 4687, 3752, K012, K024 and K045GBMs (WHO grade IV) were collected from resection [17,18]. V0914AOA xenograft passage II was kindly shared from Dr. Jialiang Wang in Vanderbilt University Medical Center, Nashville, TN, USA. Adult normal cerebra, NC2, D0322, and T0503, were obtained from autopsy. Signed informed consent was obtained from patients or legal guardian prior to sample acquisition in accordance with Institutional Review Board policy. All studies were conducted in accordance with the ethical guidelines of Declaration of Helsinki.

Growth of tumor cell cultures

Patient-derived neurosphere line of BT142AOA, xenograft cells of V0914AOA, xenograft-derived neurosphere lines of 4687 and 3752 [18] were cultured in serum-free cell growth medium, in which putative cancer stem cell populations are enriched (see Supplementary Materials and Methods).

Orthotopic PDX mouse models

Orthotopic free-hand surgical transplantation of tumor cells into mouse cerebra was performed as we have described previously [19] following an Institutional Animal Care and Use Committee-approved protocol. (see Supplementary Materials and Methods).

PCR and pyrosequencing – IDH1 (R132) and IDH2 (R172) mutation analysis

IDH1 (R132H and C) and IDH2 (R172K) mutation status was examined through pyrosequencing using specific primer pairs (see Supplementary Materials and Methods).

In vitro treatment with SYC-435

SYC-435 was designed and synthesized at Baylor College of Medicine by Dr. Yongcheng Song [13]. For *in vitro* experiments, SYC-435 was dissolved in dimethyl sulfoxide for a stock solution (20 mM). Tumor cells were exposed to SYC-435 (< 20 μ M) for 13 days. Cell viability was measured periodically using Cell Counting Kit-8 (Dojindo Molecular Technologies, Rockville, MD) [20,21].

In vivo treatment of orthotopic PDX mouse models with SYC-435 and standard therapy

Two weeks after tumor cell implantation, mice were treated with SYC-435 (15 mg/kg/day, ip, 28 days) and/or TMZ (50 mg/kg/day, oral) plus fractionated X-ray irradiation (XRT) (2 Gy/day) for 5 days to the right cerebrum (see Supplementary Materials and Methods). The mice were monitored daily until they developed signs of neurological deficit or became moribund, at which time they were euthanized and their brains removed for analysis. To test the biologic effects of treatments at the end of treatments, mice were treated with SYC-435 (15 mg/kg/day, ip, 5 or 10 days) and/or standard therapy (TMZ, 50 mg/kg/day, oral and XRT, 2 Gy/day, 5 days) beginning when neurologic symptoms were first observed. These mice were euthanized 1 h after the last treatment and their plasma and brains were harvested for analysis.

SYC-435, α -KG and 2-HG measurement

SYC-435, α -KG and 2-HG concentration in plasma and/or tumor was measured by liquid chromatography with tandem mass spectrometry (LC-MS/MS) (see Supplementary Materials and Methods).

Immunohistochemical staining (IHC)

IHC staining was performed as described previously [19–22] (see Supplementary Materials and Methods). IHC staining was assessed by combining intensity, scored as negative (–), low (+), medium (++), or strongly positive (+++), with extent of immunopositivity (percentage of positive cells).

Western hybridization

To analyze the changes of histone methylation, histones were prepared by acid-extraction and western hybridization was performed (see Supplementary Materials and Methods).

RNA sequencing (RNA-seq)

RNA was extracted using AllPrep DNA/RNA/Protein Mini Kit according to manufacturer's instructions (Qiagen) and RNA-seq was performed as we have described previously [23]. (see Supplementary Materials and Methods). The RNA-seq data were uploaded into the GEO database with access number GSE194169.

Flow cytometry (FCM)

Flow cytometry was performed as we described previously [17,19,24,25] (see Supplementary Materials and Methods).

Statistical analysis

Values were presented as mean ± standard deviation (SD). The effect of treatment on cell proliferation was analyzed with two-way analysis of variance (ANOVA). SYC-435 concentration, 2-HG and α-KG were analyzed with one-way ANOVA followed by a multiple comparison procedure (Holm-Sidak method). Animal survival times were compared through log-rank analysis. All statistical analyses were performed by using SigmaPlot 11.0 (Systat Software, Inc., San Jose, CA). $P < 0.05$ was considered statistically significant.

Results

Newly established orthotopic PDX model IC-V0914AOA with IDH1-R132C mutation

Intra-cerebral (IC)-V0914AOA xenografts established from recurrent AOA patient tumor (Table 1) was implanted to SCID mice. As shown in Fig. 1A, median survival days was 129 days in passage I and 57–75 days in passages II–V. H&E staining of paraffin-embedded brain showed

Table 1
Patient clinical course of V0914.

	Date	V0914
Age		21 y
Gender		Male
Original Path	8/1997	Grade 3 astrocytoma
Biopsy	9/1997	Stereotactic biopsy
Resection	3/1998	Resection
Path II	3/1998	Oligo with minor astrocytic component
Treatments received prior to collection of sample	1998–1999	Procarbazine, Vincristine, CCNU
Treatments received prior to collection of sample	2004–2006	Temodar, CPT-11, Radiation
Resection	3/2012	Recurrent Sample collected from resection
Final path		Grade 3 Oligo
Treatments received after collection of sample	5/2012	Avastin

massive tumor formation in the right cerebrum (Fig. 1B). Tumor take rate was ≥ 80% in all passages. H&E staining showed various size of tumor cells (Fig. 1Ca). Hemorrhage in tumor was frequently detected (Fig. 1Cb). Subsequent IHC examination validated the human origin of xenograft tumor in mouse brain (++ in > 75% cells) using human-specific mitochondria (MT) antibody (Fig. 1C and Table S1). High expression of cell proliferation marker Ki-67 (in 40–70% cells), vimentin (VIM), a marker of intermediate filament associated with poor prognosis and tumor invasion [26,27] (+++ in >75% cells) and tumor suppressor p53 (+++ in > 75% cells) were detected. Microvessel density (16.7 ± 7.3/high power field) was detected with vWF and it was higher compared to low grade glioma xenograft model (5.8 ± 1.1) [28] indicating highly active angiogenesis. While reactive astrocytes with strong GFAP positivity (+++ in > 75% of mouse cells) surrounding the tumor were detected, the GFAP expression in tumor was relatively low in intensity (+ in > 75% cells).

We then assessed mutations in IC-V0914AOA xenografts. For p53, R213 truncation (mutation frequency 20%) and I195T mutation (mutation frequency 21%) were detected (Fig. 1D). This may explain the high expression of TP53 protein. In addition, Q472H mutation in KDR (mutation frequency 54%) was also detected. Most importantly, an IDH1-R132C mutation (G to A transition in antisense codon 132 of IDH1 and remaining G, Fig. 1E) was detected and mutant allele frequency was maintained 39–53% in passage I–V (Figs. 1E and S1C). An IDH1-R132H mutation (C to T transition in antisense codon 132 of IDH1, Fig. S1A) was detected in BT142AOA-neurosphere and xenografts with mutant allele frequency > 94% (Fig. S1B and C) as previously reported [16]. IDH2-R172K mutation was not detected in any models (Fig. S1B and C). Taken together, IC-V0914AOA possessed high and stable tumor take rate as well as histopathological feature and mutation status consistent with a human high-grade glioma, representing a suitable model for pre-clinical drug testing targeting the IDH1-R132C mutation.

SYC-435 selectively inhibited cell proliferation in IDH1 mutant glioma cells

The structure of SYC-435 (MW:215.3) was shown in Fig. 2A. A time- and dose-dependent inhibition of cell proliferation under SYC-435 treatment was observed (Fig. 2B and C). SYC-435 at 0.5 and 1 μM suppressed cell proliferation 85.9% and 99.5%, respectively, in BT142AOA-neurospheres (R132H) at Day 13. Similarly, in IC-V0914AOA xenograft cells (R132C), SYC-435 at 0.5 and 1 μM suppressed cell proliferation 59% and 99.3%, respectively at Day 13. No major difference in inhibition of cell proliferation between R132H and R132C mutant lines was consistent with the inhibitory effect of SYC-435 in IDH enzyme activity [29]. In IDH1-WT 4687 and 3752GBM-neurospheres, 0.5 μM inhibited < 15% and 1 μM only up to 60.0% and 77.2% growth suppressions on day 13, respectively. Overall, SYC-435 preferentially inhibited cell proliferation in IDH1 mutant glioma with lower doses and/or shorter incubation times cells over IDH1-WT GBM cells, exhibiting approximately 2-fold differences.

Combining SYC-435 with standard therapy synergistically prolonged animal survival time

Next, we investigated the *in vivo* therapeutic efficacy, survival benefits, of SYC-435 combined with standard therapy (TMZ/XRT) (Fig. 3A). The orthotopically implanted GBM tumor cells were allowed to grow for 2 weeks to form solid intra-cerebral xenografts before treatment were started with SYC-435 (15 mg/kg, i.p, daily x 28 days), XRT (2 Gy/day x 5 days) and TMZ (50 mg/kg, i.p., daily x 5 days). In IC-V0914AOA, SYC-435 only increased the median survival times from 77 days in control to 82 days ($P > 0.05$), while TMZ/XRT significantly extended to 106 days compared to control ($P < 0.0005$). The combination (SYC-435/TMZ/XRT) further prolonged the median survival time to 124 days, a 61% increase over the control ($P < 0.00005$), 16.9% prolongation over the

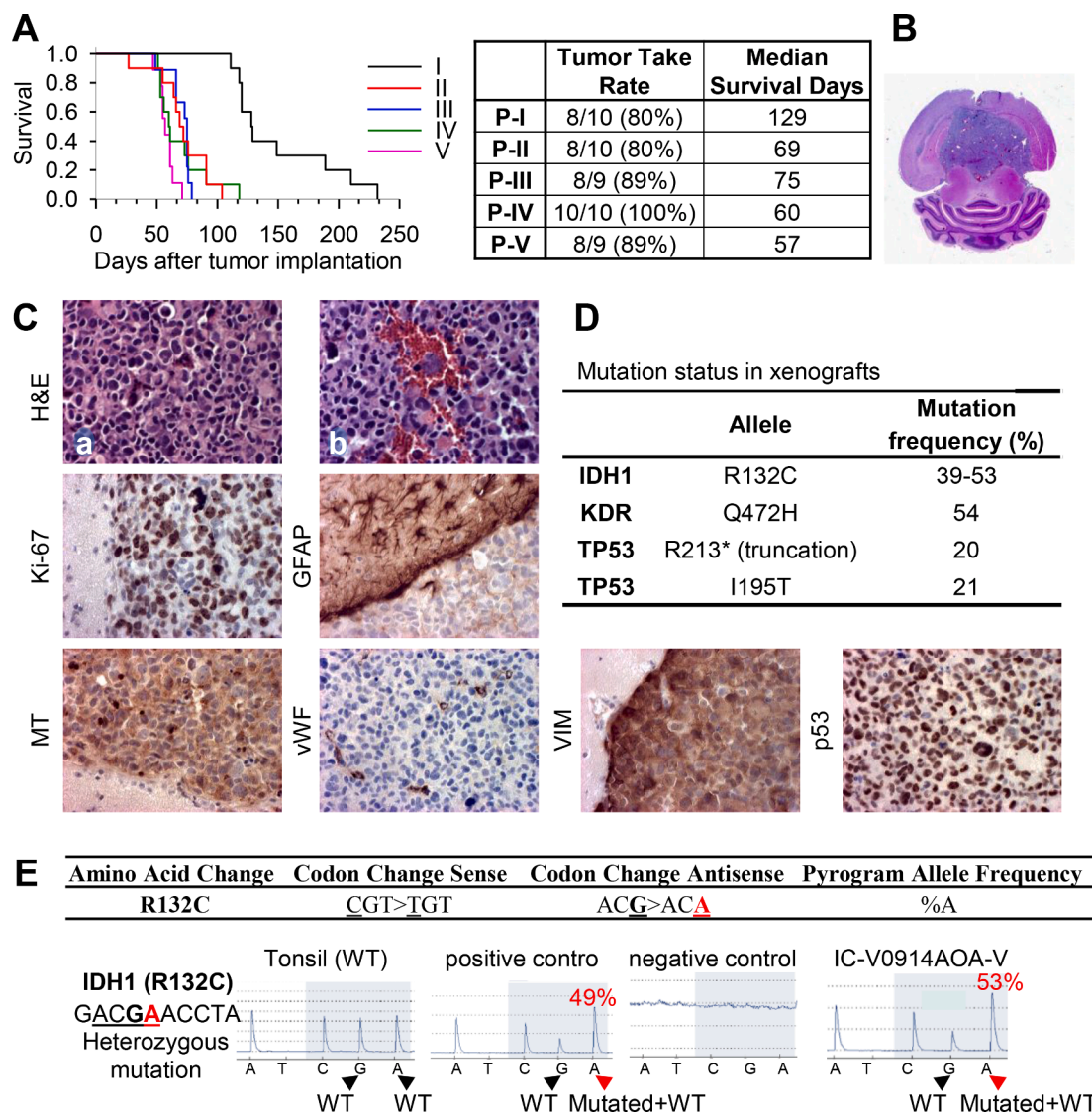


Fig. 1. Establishment of IC-V0914AOA, orthotopic PDX mouse model with mutant IDH1-R132C. (A) Log-rank analysis of animal survival times during serial sub-transplantation of IC-V0914AOA from passage I to V (left panel). Tumor take rate median survival days (right panel). (B) H&E stained cross section of IC-V0914AOA. (C) Histopathological features of IC-V0914AOA. Representative H&E staining of mouse brain shows tumor cell morphology (a) and hemorrhage in tumor (b). Representative IHC staining shows tumor cells positively stained with Ki-67, vimentin (VIM), p53, GFAP, reactive mouse astrocytes (monoclonal antibodies against GFAP) and blood vessels (bv) with vWF. Human tumor cells confirmed with human-specific antibodies against mitochondria (MT). Magnification x40. (D) Mutation status in IC-V0914AOA xenografts. (E) Quantitative analysis of IDH1-R132C mutation allele frequency using pyrosequencing. Codon change in IDH1-R132C, representative pyrograms indicating G (WT) to A (mutated) substitution in percent for IC-V0914AOA was indicated.

TMZ/XRT ($P < 0.05$), demonstrating a synergistic activity when SYC-435 is combined with the standard therapies. In IC-BT142AOA, the median survival time of 85 days in SYC-435 was barely increased from the control of 82 days ($P > 0.05$). TMZ/XRT significantly prolonged the survival time to 177 days ($P < 0.0001$). SYC-435/TMZ/XRT further prolonged to 205 days, but the difference with TMZ/XRT groups was not significant ($P > 0.05$). The strong efficacy of TMZ/XRT in IC-BT142AOA, *i.e.*, 115% increase of survival time over the control, may have made it difficult for further extension. Altogether, our data demonstrated strong and synergistic *in vivo* anti-tumor activity of SYC-435 with standard therapies.

SYC-435 effectively crossed BBB to penetrate orthotopic xenograft tumors

We examined the CNS penetration capability of SYC-435 to determine if the synergy with TMZ/XRT was due to the improved drug delivery by the standard therapies in IC-V0914AOA (Fig. 3B). After SYC-

435 single agent treatment for 5 or 10 days, its concentration in tumors ranged from 154 ± 36 to 185 ± 42 ng/g (Fig. 3C). Similar SYC-435 levels were achieved when combined with TMZ/XRT. Compared with the plasma concentration of SYC-435 (213 ± 8 to 258 ± 56 ng/mL) by the treatment of SYC-435 with/without TMZ/XRT for 5 and 10 days, tumor penetration reached 67–79% (Fig. 3C). These data confirmed SYC-435 successfully crosses the BBB and maintained stable levels in tumors after 5 days and TMZ/XRT did not significantly affect SYC-435 penetration into brain tumors.

SYC-435 induced modification of histone methylation

We measured concentrations of α -KG and oncometabolite 2-HG, a competitive inhibitor of α -KG-dependent dioxygenases [4]. 2-HG concentration was dramatically increased to 54.3 ± 11.7 mg/g in untreated IC-V0914AOA compared to IDH1-WT tumors (0.5 ± 0.1 mg/g) ($P < 0.005$) (Fig. 3D). None of the treatments changed 2-HG level. Despite

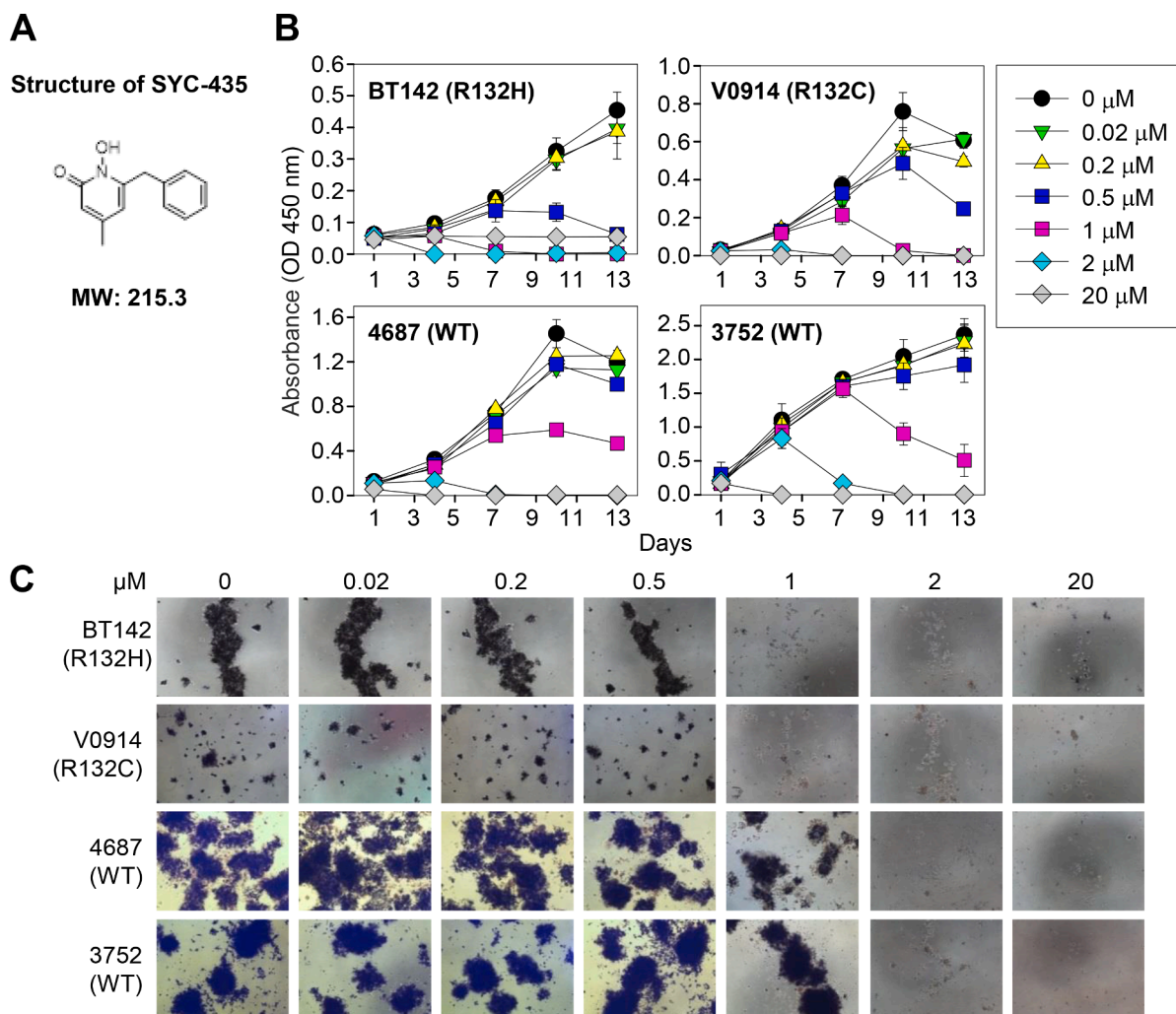


Fig. 2. Anti-tumor effects of SYC-435 in glioma cells. (A) Structure and molecular weight of investigational mutant IDH1 inhibitor, SYC-435. (B) Cells (2000–6000 cells/well) were exposed to SYC-435 for 13 days and anti-tumor effects were examined by Cell Counting Kit-8 assay in BT142-neurosphere (R132H), IC-V0914AOA xenograft cells (R132C), 4687GBM-neurosphere and 3752GBM-neurosphere (WT). (C) Anti-tumor effect was observed by staining with 250 μg/mL of MTT for 4 h at Day 11. Viable cells were stained with dark colored intracellular crystal.

the presence of an IDH1-R132C mutation, α -KG concentration in untreated IC-V0914AOA was not reduced compared to IDH1-WT tumors and none of the treatments changed α -KG concentration (Fig. 3D).

2-HG inhibits histone demethylases, resulting in hypermethylation of histone lysine residues (especially in H3) [30]. We next investigated the histone H3 lysine methylation status. As shown in Fig. 3E, protein levels of H3K4me2 and H3K4me3 as well as H3K9me2 and H3K9me3, H3K36me3, H3K79me2 and H3K79me3 were increased in both IC-V0914AOA and IC-BT142AOA tumors compared with IC-K012GBM (WT). Although TMZ/XRT did not affect their expression, SYC-435 caused a dose-dependent decrease of H3K4me2, H3K4me3, H3K9me2 and H3K9me3 expression in IC-V0914AOA on day 5. In addition, SYC-435 with TMZ/XRT synergistically decreased those levels. Prolonged treatment to 10 days was only able to generate sustained suppression of H3K4me2 and H3K9me2, while protein expression of H3K4me3 and H3K9me3 was restored back to the high levels. Surprisingly, combining SYC-435 with TMZ/XRT lead to a sustained reduction of H3K4me3 and H3K9me3, particularly at 30 mg/kg. Since all the tumors eventually recurred in the survival group and the recurrent tumor regained the high levels of H3K4me3 and H3K9me3 as well as H3K4me2, sustained inhibition of H3K4me3, H3K9me3 and H3K4me2 by SYC-435/TMZ/XRT may have contributed to the synergistic therapeutic efficacy *in vivo*.

Acute treatment with SYC-435 and/or standard therapy affected different gene sets

To further understand the acute changes of gene expression profiles directly induced by treatments, we performed RNA-seq analysis in tumors from biology cohort (Fig. 3B) of IC-V0914AOA. Compared with untreated tumor, SYC-435 up-regulated 596 and down-regulated 1561 genes. Notably, 22 of the top 30 (73%) up-regulated genes by SYC-435 were mitochondrial genes. Mitochondrial genes were significantly down-regulated in SYC-435/TMZ/XRT group both in the biology and survival cohorts (Fig. S2). TMZ/XRT up-regulated 81 and down-regulated 272 genes with 33 genes jointly up-regulated (including 12 mitochondrial genes) and 127 genes jointly inhibited with SYC-435 group. SYC-435/TMZ/XRT affected the least number of genes, activating 38 and inhibiting 23 genes with < 10 genes shared with either SYC-435 or TMZ/XRT groups (Fig. 4A, left panel). These data suggested that SYC-435 and standard therapy target distinct sets of genes with limited overlap.

Hierarchical clustering analysis of the top 30 up-/down-regulated genes of all the treatment groups in the biology cohort showed SYC-435 was most active in reversing the dysregulated genes of the untreated tumors (Fig. 4B, left panel), inhibiting the expression of nestin (NES), VGF, PARP1, and SET Domain bifurcated histone lysine

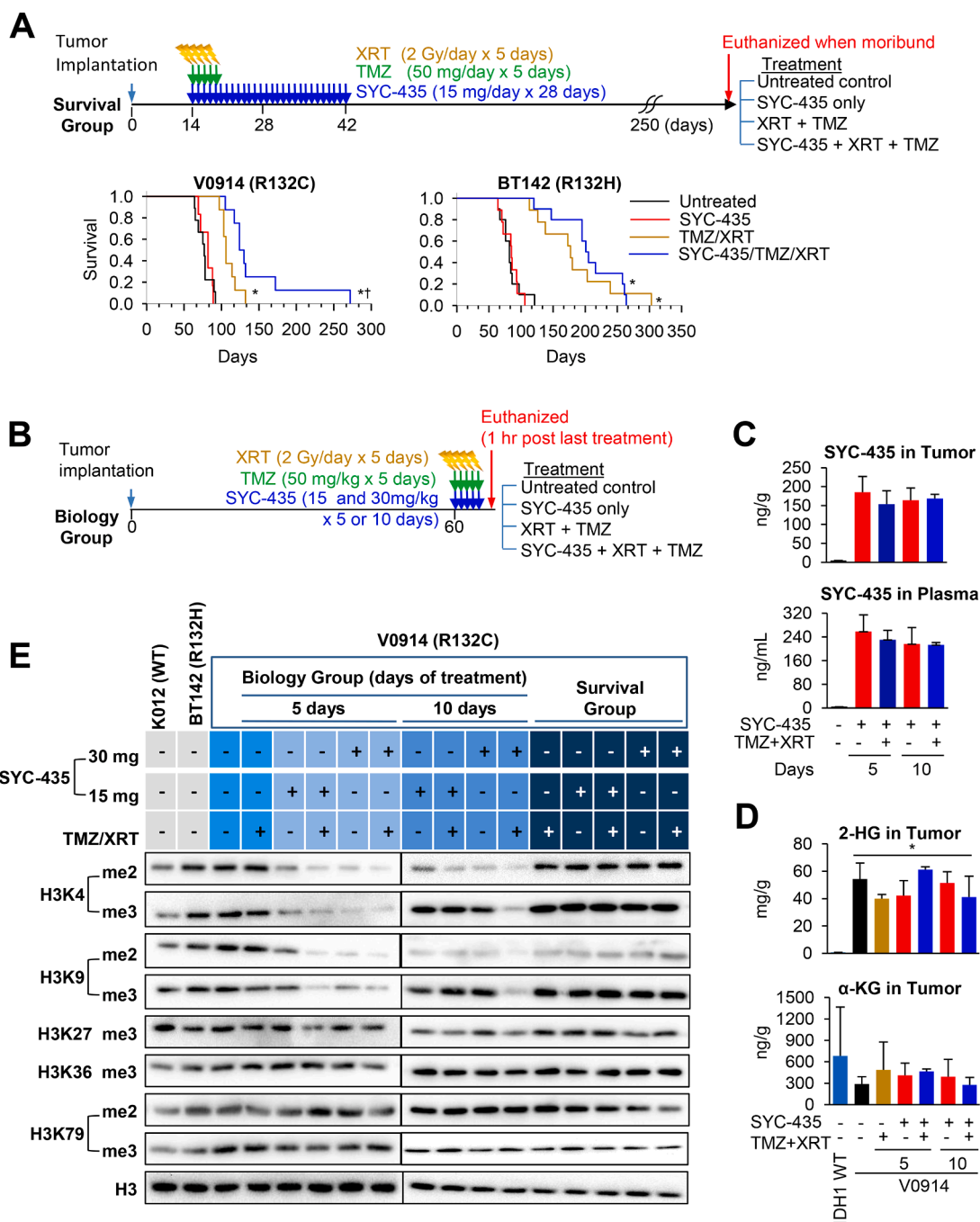


Fig. 3. SYC-435 can penetrate into mouse brains and prolongs animal survival in combination with standard therapy in IC-V0914AOA (R132C) but not in IC-BT142AOA (R132H). (A) Two weeks after tumor implantation, mice were treated with SYC-435 and/or standard therapy (TMZ/XRT) as indicated in A (Survival group). Animal survival was monitored. $n = 10$ per group. $*P < 0.0005$ compared to Untreated, $^{\dagger}P < 0.05$ compared to TMZ/XRT. (B) After early signs of sickness were observed in IC-V0914AOA, mice were treated with SYC-435 and/or standard therapy as indicated in B (Biology group). Plasma and tumor were obtained at 1 h after the last treatment and SYC-435 (C), 2-HG and α -KG concentration (D) in IC-V0914AOA were measured by LC-MS/MS. $*$, $P < 0.005$ compared to IDH1-WT. (E) Histone methylation in IC-V0914AOA was detected by western hybridization.

methyltransferase 1 (*SETDB1*) and activating *ITGB8*, *CD34* (angiogenesis marker), *MYO1F*, *ICAM2*, and *BLCAP* (an apoptosis inducing factor). Ingenuity analysis also identified 8 pathways that were commonly modulated by all treatments in the biology cohort (Fig. 4C and Table S2). Two of these pathways, the sirtuin signaling pathway and the protein ubiquitination pathway, were also shared in the survival cohort in which the total number of the affected signaling pathway was much smaller (Fig. 4C and Table S3).

Molecular mechanisms of recurrence and potential novel therapeutic targets

To investigate the molecular causes of recurrence, RNA-seq was performed in the recurrent/remnant tumors (survival cohort). In the tumors of the survival cohort, SYC-435 up-regulated 374 (> 2 fold) and down-regulated 735 genes, while TMZ/XRT up-regulated 51 and down-regulated 16 genes, and SYC-435/TMZ/XRT activated 47 and suppressed 37 genes compared with untreated tumor (Fig. 4A, right panel). Hierarchical clustering analysis of the top 30 up-/down-regulated genes

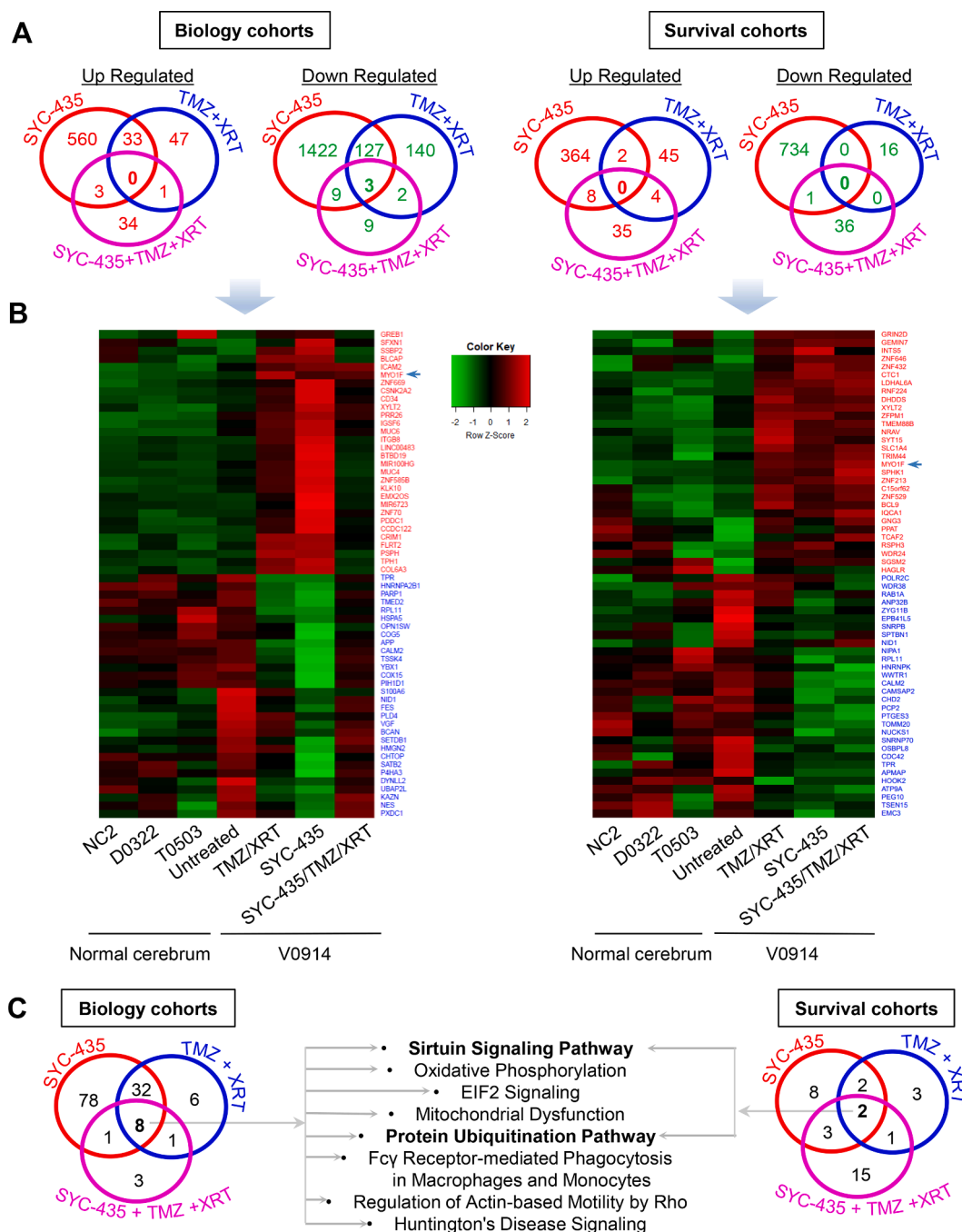


Fig. 4. Identification of molecules regulated by SYC-435 and standard therapy. IC-V0914AOA mice were treated with SYC-435 (15 mg/kg/day) and/or standard therapy for treatment schedules of biology (5 days) and survival cohorts. RNA extraction/RNA-seq analysis was performed. (A) Summary of up- and down-regulated genes as related to the three different treatment strategies compared to untreated control. (B) Heatmaps show top 30 up (red)- and down (blue)-regulated molecules induced by the treatments compared to untreated control. (C) Summary of the affected signaling pathways with p -value < 0.01 (equal to $-\log_{10}(p\text{-value}) > 2$) compared to untreated control. Shared pathways were highlighted.

revealed significant differences between the recurrent tumors (in all three treatment groups) and the untreated tumor (Fig. 4B, right panel). The activated (e.g., *BCL9*, *CTC1*, *MYO1F*) and down-regulated genes (e.g., *CDC42*, *HOOK2*, *PEG10*, *RAB1a*) were largely different from those in the biological cohort. *MYO1F* was the only gene that was activated by all the treatments in the biology cohorts and remained elevated in the survival cohorts (Fig. 4B). These data showed that SYC-435 and/or the standard therapy significantly altered the overall gene expression profile of the IC-V0914AOA tumors, which in turn confirmed the dramatic genetic differences between primary and recurrent tumors.

To identify pathways that promoted recurrence in the survival

cohorts after the treatments were discontinued, significantly altered pathways in survival cohort compared to biology cohort were detected (Fig. 5 and Table S4). The differentially expressed genes ($|\text{fold change}| \geq 2$) were analyzed by Ingenuity Pathway Analysis (IPA). The canonical pathways with most over represented genes are obtained by pathway enrichment analysis with $-\log_{10}(P\text{-Value}) > 1.32$ (Fisher's exact test). Many of the affected signaling pathways ($n = 110$) in SYC-435 group were altered when the treatment was discontinued indicating short-term effects or reversible activities of SYC-435. Changes induced by the TMZ/XRT and SYC-435/TMZ/XRT groups were more sustainable as only 13 pathways found in the acute treatment phase

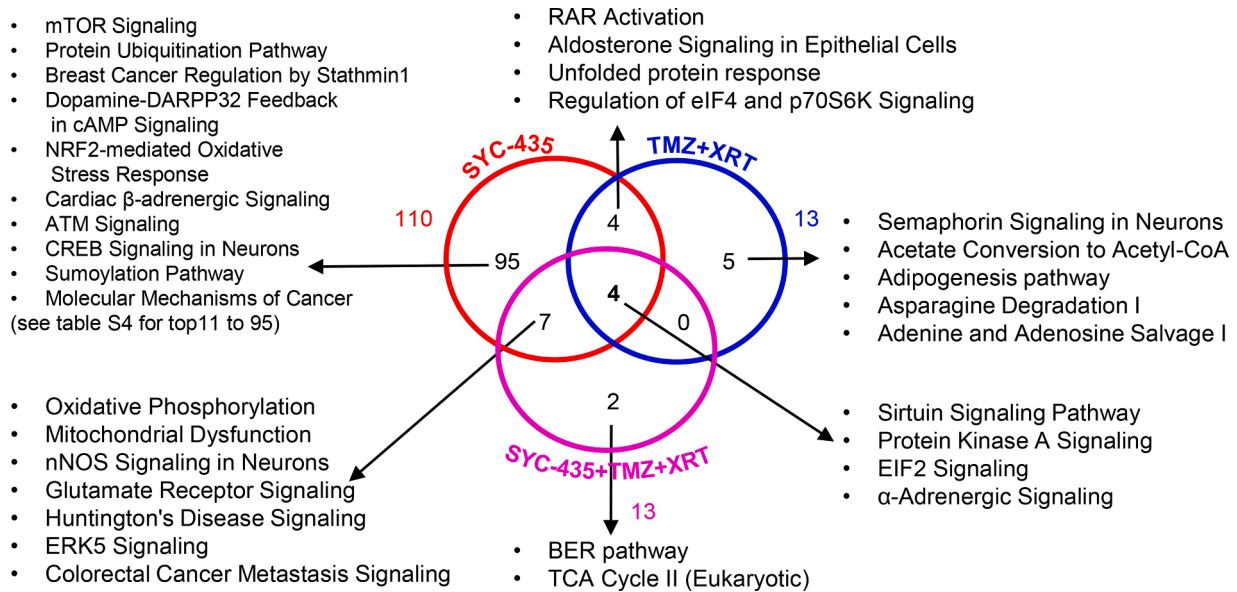


Fig. 5. Private and shared signaling pathways among the treatments that were contributed to tumor resistance/recurrence. IC-V0914AOA mice were treated with SYC-435 (15 mg/kg/day) and/or standard therapy for treatment schedules of biology (5 days) and survival cohorts. RNA extraction/RNA-seq analysis was performed. Pathways with p -value < 0.01 (equal to $-\log_{10}(p\text{-value}) > 2$) in biology cohort vs survival cohort in each treatment was analyzed. Private and shared signaling pathways were identified.

were altered in the recurrent tumors (Fig. 5 and Table S4) indicating that the standard therapy may have played a dominant role in sustaining the combination treatment induced genetic changes. These pathways altered by the combination therapy may have contributed to tumor recurrence. Among them, the base excision repair (BER) and TCA cycle II pathways occurred exclusively in SYC-435/TMZ/XRT group, while 4 pathways (sirtuin signaling, protein kinase A, eukaryotic initiation factor 2 (EIF2) and α -adrenergic signaling) were shared by all three treatments (Fig. 5 and Table S4). These data provided important clues to inform future molecular targets for the development of therapies for tumor recurrence. For example, the expression of G protein subunit gamma 3 (*GNG3*), one of hub genes recently found in GBM [31], was significantly increased following SYC-435/TMZ/XRT compared to untreated IC-V0914AOA at the end of treatment (biology cohort) and it sustained in recurrent tumors (survival cohort). *GNG3* was down-regulated ($\log_2(\text{fold change}) = -0.72$) in untreated IC-V0914AOA compared to normal tissue (Tables S5–8).

Impact of the combined therapy on cancer stem cells and cellular apoptosis

Since we have observed the down-regulation of nestin, a gene frequently associated with cancer stem cells (CSCs) [32], we examined the contribution of CSCs to the effect of therapies. IC-V0914AOA and IC-BT142AOA showed low levels of CD133/CD15 expression and neither SYC-435 nor TMZ/XRT treatment changed CD133/CD15 expression in biology/survival groups (Fig. S3). We also examined whether survival benefits were mediated by apoptosis. IHC staining showed SYC-435 and TMZ/XRT treatment in IC-V0914AOA did not increase the levels of the cleaved caspase-3 and cleaved PARP (+++ in $\leq 25\%$ cells or ++ in $\leq 25\%$ cells in any treatment groups at any time points) (Table S1). Taken together, these data suggested the survival benefits were independent of CSC expression and apoptosis.

Discussion

In this study, we established a novel AOA orthotopic PDX mouse model, IC-V0914AOA, the first glioma xenograft model with IDH1-R132C mutation. This model possessed high and stable tumor take rate. Histopathological and molecular feature and mutation status were

consistent with a human high-grade glioma, representing a suitable model for pre-clinical drug testing targeting the IDH1-R132C mutation. The mutant protein IDH1-R132C also produced 2-HG similar to IDH1-R132H [7]. Therefore, this model not only represents patients with R132C mutation (3.7–4.3% of glioma) [6,7], but also contributes to the cohort of xenografts with IDH1 mutation. TP53 mutation frequently co-occurred with IDH1 mutation [33,34], and our IC-V0914AOA harbors a TP53 mutation as well as *IDH1*.

Effective delivery of therapeutic agents across the BBB has long been a challenge for brain tumor treatment. Compared with other existing IDH1 inhibitors, our newly developed SYC-435 has the smallest MW. Although SYC-435's IC_{50} inhibition of 2-HG ($2.4 \pm 0.5 \mu\text{M}$) in human fibrosarcoma HT1080 cells (R132C) [29] was higher than AG-120 ($0.039 \mu\text{M}$), AGI-5198 ($0.724 \mu\text{M}$) [14], and MRK-A ($0.1 \mu\text{M}$) [12], SYC-435 at $0.5 \mu\text{M}$ suppressed cell proliferation $>50\%$ in BT142AOA and V0914AOA, which was better than the 30% cell growth inhibition by $50 \mu\text{M}$ of AGI-5198 in IDH1-R132H mutant cells [35] and no changes in cell viability were observed by $1 \mu\text{M}$ of MRK-A [12]. Using our orthotopic PDX models, we confirmed that SYC-435 was able to effectively penetrate the orthotopic PDX tumors and such drug delivery was not adversely affected by the standard therapy.

More importantly, SYC-435 significantly prolonged animal survival times when combined with standard therapy. Although SYC-435 penetrated the BBB, SYC-435 alone did not improve survival, which was similar to other investigational mutant IDH1 inhibitors acting alone [11]. While it is frequently accepted that combination therapy leads to better therapeutic outcomes in most tumors, it is often challenging to select proper combinatory treatment. Since patients with high grade gliomas harboring IDH1 mutation often have better overall survival than those with IDH1-WT tumor when treated with radiation alone or in combination with TMZ [36] and GBM cells overexpressing IDH1-R132H and IDH2-R172K mutant proteins displayed higher radiation sensitivity *in vitro* [37], we decided to combine SYC-435 with the standard therapy of XRT and TMZ. Remarkably, such combination significantly prolonged animal survival time compared to standard therapy alone in IC-V0914AOA. Our data demonstrated of synergistic activities of this combination supports the translation of SYC-435 into clinical trials.

To address the underlying mechanism of action of SYC-435, we measured 2-HG and α -KG levels and histone H3 lysine methylations.

Although IDH1-R132C mutation in IC-V0914AOA dramatically increased 2-HG level, SYC-435 treatment with/without standard therapy did not significantly suppress 2-HG. This finding combined with our *in vitro* observation and comparison with other IDH1 inhibitors (as mentioned above) supports that 2-HG levels should not be used to evaluate the anti-tumor activities of mutant IDH1 inhibitors. In contrary, SYC-435 treatment with/without standard therapy dramatically reduced methylation of H3K4 and H3K9. Hypermethylation of H3K4 and H3K9 results in tumorigenesis, de-differentiation and drug resistance [38]. Thus, the down-regulated H3K4 and H3K9 methylation might have contributed significantly to the anti-tumor effects of SYC-435. In addition, our analysis of the putative CSCs did not identify major changes of CD133⁺/CD15⁺ cell fraction suggesting the SYC-435 and standard therapy combination was effective in killing both cancer stem and non-stem tumor cells.

Our RNA-seq data also shed light to the mechanism of xenograft survival prolongation. Interestingly, compared to SYC-435 alone, standard therapy affected less genes/pathways, combination therapy (SYC-435/TMZ/XRT) affected the least genes/pathways in biology cohort and survival outcome was the best. Acute treatment of SYC-435-induced changes were short-term effects or reversible. The standard therapy may have played a dominant role in sustaining the combination treatment induced genetic changes. The dramatic genetic differences between primary and recurrent tumors were confirmed. We identified that *MYO1F* was the only gene that was activated by all the treatments immediately at the end of treatments (biology cohorts) and remained elevated until tumor relapse (survival cohorts). Interestingly, mutant *MYO1F* was recently shown to alter the mitochondrial network and induces tumor proliferation in thyroid cancer [39]. B-cell lymphoma 9 (*BCL9*) and conserved telomere maintenance component 1 (*CTC1*) were activated by all the treatments in recurrent tumor. It was reported that loss of *BCL9* blocks colonic tumorigenesis [40]. *CTC1* increases the radioresistance of human melanoma cells by inhibiting telomere shortening and apoptosis [41]. These indicate tumor-activating molecules were up-regulated in recurrent tumors. Signaling pathways contributed to tumor resistance/recurrence in combination therapy were in the wide range. BER pathway which was reported that blocking BER enhanced response to TMZ [42]; protein kinase A were ten-times more abundant in GBM than normal brain, protein kinase A was involved in differentiation and apoptosis in glioma cells [43,44]; TCA cycle II and sirutin signaling pathway (mitochondria and mtDNA); EIF2 signaling (angiogenesis); indicating there are wide range of targets to completely suppress recurrence. Among identified genes and pathways by RNA-seq in this study, regulation of nestin has been also reported after the treatment of other mutant IDH1 inhibitors. AGI-5198 treatment markedly reduced the fraction of nestin-positive TS603 cells *in vitro* [11]. In contrast, MRK-A treatment increased nestin expression in BT142 cells *in vitro*. MRK-A treatment *in vivo* did not change nestin levels [12]. In our study, SYC-435 down-regulated nestin expression in biology cohort in IC-V0914AOA. Mutant IDH1 inhibitors works differently for nestin in different IDH1-mutated cells indicating nestin is not crucial target of mutant IDH1 inhibitors. To date, a high frequency of mtDNA mutations and copy numbers in GBM patients [45,46] and increased tumor mtDNA content in IDH1-mutant low grade gliomas [47] as well as reduction of mtDNA transcription in GBM [48] have been reported. In the current study, we found 22 of the 30 (73%) top up-regulated genes by SYC-435 were mitochondrial genes compared to untreated tumor. Combination therapy down-regulated mtDNA-encoded molecules at the end of treatment and recurrent tumor, which seemed to agree with a previous study in which depleting mtDNA in GBM cells decreased their tumor forming capacity *in vivo* [49]. Notably, there were changes in mtDNA-encoded molecules and H3K4/H3K9 methylation (e.g., K3K4me2, K3K4me3, H3K9me2 and H3K9me3) which played key roles in mediating SYC-435-induced anti-tumor activities. Our RNA-seq analysis showed that *GNG3* expression was up-regulated in combination therapy compared to the untreated control both at the end of

treatment and recurrent samples. As seen in our experiments, down-regulation of *GNG3* in GBM has also been reported [31]. This is the only molecule consistently up-regulated both at the end of treatment and at recurrence, although the full contribution of *GNG3* in GBM remains to be elucidated.

In conclusion, we have newly established and characterized an orthotopic PDX mouse model of IC-V0914AOA bearing IDH1-R132C mutation. Inhibition of mutant IDH1 by SYC-435 decreased growth of both IDH1 mutant and WT glioma *in vitro* but not *in vivo*. SYC-435 treatment synergistically prolonged animal survival in combination with standard therapy. Therapeutic agents targeting the regulation of H3K4/H3K9 methylation, *MYO1F*, *CTC1*, *BCL9* and mtDNA-encoded molecules should be prioritized as targets for further mechanism characterization. Our data support the rationale for SYC-435 in clinical trial testing for patients with IDH1 mutant glioma treated with standard therapy.

CRediT authorship contribution statement

Mari Kogiso: Conceptualization, Validation, Formal analysis, Investigation, Writing – original draft, Visualization, Project administration, Writing – review & editing. **Lin Qi:** Validation, Investigation, Resources, Writing – review & editing, Project administration. **Yuchen Du:** Methodology, Validation, Investigation, Writing – review & editing, Project administration. **Frank K. Braun:** Methodology, Validation, Investigation, Writing – review & editing. **Huiyuan Zhang:** Validation, Investigation, Writing – review & editing. **L. Frank Huang:** Validation, Formal analysis, Investigation, Writing – review & editing, Funding acquisition. **Lei Guo:** Validation, Investigation, Writing – review & editing. **Yulun Huang:** Investigation, Writing – review & editing. **Wan-Yee Teo:** Formal analysis, Writing – review & editing, Funding acquisition. **Holly Lindsay:** Investigation, Writing – review & editing, Funding acquisition. **Sibo Zhao:** Investigation, Writing – review & editing. **Sarah G. Injac:** Investigation, Writing – review & editing. **Zhen Liu:** Resources, Writing – review & editing. **Vidya Mehta:** Validation, Investigation, Writing – review & editing. **Diep Tran:** Validation, Investigation, Writing – review & editing. **Feng Li:** Methodology, Writing – review & editing, Funding acquisition. **Patricia A. Baxter:** Validation, Writing – review & editing. **Jack M. Su:** Validation, Writing – review & editing. **Laszlo Perlaky:** Resources, Writing – review & editing. **D. Williams Parsons:** Validation, Writing – review & editing. **Murali Chintagumpala:** Validation, Writing – review & editing. **Adekunle Adesina:** Validation, Writing – review & editing. **Yongcheng Song:** Conceptualization, Resources, Writing – review & editing, Funding acquisition. **Xiao-Nan Li:** Conceptualization, Methodology, Validation, Formal analysis, Investigation, Resources, Writing – original draft, Writing – review & editing, Visualization, Supervision, Project administration, Funding acquisition.

Declaration of Competing Interest

The authors declare that they have no known competing financial interests or personal relationships that could have appeared to influence the work reported in this paper.

Acknowledgements

Xiao-Nan Li is funded by NIH RO1 CA185402, 1-UO1-CA217613, and Cancer Prevention and Research Institute of Texas (CPRIT) RP150032, RP170169; Yong-Cheng Song by CPRIT RP140469 and RP180177, NIH/NINDS RO1 NS080963; Holly Lindsay by the Chance for Hope Foundation Career Development Award; Wan-Yee Teo by SingHealth @ Institute of Molecular and Cell Biology Program Grant (W. Y.T) and the National Medical Research Council Singapore, Clinician Scientist Award; Feng Li by CPRIT Core Facility Support Award (RP160805) and Welch Foundation Grant (H-Q-0042) for support of

NMR and Drug Metabolism Core at Baylor College of Medicine operations; L. Frank Huang (L.F.H) by CancerFree KIDS Foundation Fund, Research, Innovation & Pilot (RIP) Funding Awards from Cincinnati Children's Research Foundation, and start-up funding support from the Division of Experimental Hematology and Cancer Biology, Brain Tumor Center, Cincinnati Children's Hospital Medical Center. We appreciate Dr. Jialiang Wang in Vanderbilt University Medical Center, Nashville, TN, USA to kindly share V0914AOA xenograft cells.

Supplementary materials

Supplementary material associated with this article can be found, in the online version, at doi:10.1016/j.tranon.2022.101368.

References

- [1] R.J. Haselbeck, L. McAlister-Henn, Function and expression of yeast mitochondrial NAD- and NADP-specific isocitrate dehydrogenases, *J. Biol. Chem.* 268 (1993) 12116–12122.
- [2] G.T. Jennings, S. Sechi, P.M. Stevenson, R.C. Tuckey, D. Parmelee, L. McAlister-Henn, Cytosolic NAD(+) dependent isocitrate dehydrogenase. Isolation of rat cDNA and study of tissue-specific and developmental expression of mRNA, *J. Biol. Chem.* 269 (1994) 23128–23134.
- [3] L. Dang, D.W. White, S. Gross, B.D. Bennett, M.A. Bittinger, E.M. Driggers, V. R. Fantin, H.G. Jang, S. Jin, M.C. Keenan, K.M. Marks, R.M. Prins, P.S. Ward, K. E. Yen, L.M. Liaw, J.D. Rabinowitz, L.C. Cantley, C.B. Thompson, M.G. Vander Heiden, S.M. Su, Cancer-associated IDH1 mutations produce 2-hydroxyglutarate, *Nature* 462 (2009) 739–744.
- [4] W. Xu, H. Yang, Y. Liu, Y. Yang, P. Wang, S.H. Kim, S. Ito, C. Yang, P. Wang, M. T. Xiao, L.X. Liu, W.Q. Jiang, J. Liu, J.Y. Zhang, B. Wang, S. Frye, Y. Zhang, Y. H. Xu, Q.Y. Lei, K.L. Guan, S.M. Zhao, Y. Xiong, Oncometabolite 2-hydroxyglutarate is a competitive inhibitor of alpha-ketoglutarate-dependent dioxygenases, *Cancer Cell* 19 (2011) 17–30.
- [5] H. Yan, D.W. Parsons, G. Jin, R. McLendon, B.A. Rasheed, W. Yuan, I. Kos, I. Batinic-Haberle, S. Jones, G.J. Riggins, H. Friedman, A. Friedman, D. Reardon, J. Herndon, K.W. Kinzler, V.E. Velculescu, B. Vogelstein, D.D. Bigner, IDH1 and IDH2 mutations in gliomas, *N. Engl. J. Med.* 360 (2009) 765–773.
- [6] L.A. Gravendeel, N.K. Kloosterhof, L.B. Bralten, R. van Marion, H.J. Dubbink, W. Dinjens, F.E. Bleeker, C.C. Hoogenraad, E. Michiels, J.M. Kros, M. van den Bent, P.A. Smitt, P.J. French, Segregation of non-p.R132H mutations in IDH1 in distinct molecular subtypes of glioma, *Hum. Mutat.* 31 (2010) E1186–E1199.
- [7] S. Pusch, L. Schweizer, A.C. Beck, J.M. Lehmler, S. Weissert, J. Balss, A.K. Miller, A. von Deimling, D-2-Hydroxyglutarate producing neo-enzymatic activity inversely correlates with frequency of the type of isocitrate dehydrogenase 1 mutations found in glioma, *Acta Neuropathol. Commun.* 2 (2014) 19.
- [8] D.W. Parsons, S. Jones, X. Zhang, J.C. Lin, R.J. Leary, P. Angenendt, P. Mankoo, H. Carter, I.M. Siu, G.L. Gallia, A. Olivi, R. McLendon, B.A. Rasheed, S. Keir, T. Nikolskaya, Y. Nikolsky, D.A. Busam, H. Tekleab, L.A. Diaz, J. Hartigan, D. R. Smith, R.L. Strausberg, S.K. Marie, S.M. Shinjo, H. Yan, G.J. Riggins, D. D. Bigner, R. Karchin, N. Papadopoulos, G. Parmigiani, B. Vogelstein, V. E. Velculescu, K.W. Kinzler, An integrated genomic analysis of human glioblastoma multiforme, *Science* 321 (2008) 1807–1812.
- [9] T. Watanabe, S. Nobusawa, P. Kleihues, H. Ohgaki, IDH1 mutations are early events in the development of astrocytomas and oligodendrogliomas, *Am. J. Pathol.* 174 (2009) 1149–1153.
- [10] H. Ohgaki, P. Kleihues, The definition of primary and secondary glioblastoma, *Clin. Cancer Res.* 19 (2013) 764–772.
- [11] D. Rohle, J. Popovici-Muller, N. Palaskas, S. Turcan, C. Grommes, C. Campos, J. Tsoi, O. Clark, B. Oldrini, E. Komisopoulou, K. Kunii, A. Pedraza, S. Schalm, L. Silverman, A. Miller, F. Wang, H. Yang, Y. Chen, A. Kernysky, M.K. Rosenblum, W. Liu, S.A. Biller, S.M. Su, C.W. Brennan, T.A. Chan, T.G. Graeber, K.E. Yen, I. K. Mellinger, An inhibitor of mutant IDH1 delays growth and promotes differentiation of glioma cells, *Science* 340 (2013) 626–630.
- [12] J. Kopinja, R.S. Sevilla, D. Levitan, D. Dai, A. Vanko, E. Spooner, C. Ware, R. Forget, K. Hu, A. Kral, P. Spacciapoli, R. Kennan, L. Jayaraman, V. Pucci, S. Perera, W. Zhang, C. Fischer, M.H. Lam, A brain penetrant mutant IDH1 inhibitor provides *in vivo* survival benefit, *Sci. Rep.* 7 (2017) 13853.
- [13] B. Zheng, Y. Yao, Z. Liu, L. Deng, J.L. Anglin, H. Jiang, B.V. Prasad, Y. Song, Crystallographic investigation and selective inhibition of mutant isocitrate dehydrogenase, *ACS Med. Chem. Lett.* 4 (2013) 542–546.
- [14] D.J. Urban, N.J. Martinez, M.I. Davis, K.R. Brimacombe, D.M. Cheff, T.D. Lee, M. J. Henderson, S.A. Titus, R. Pragni, J.M. Rohde, L. Liu, Y. Fang, S. Karavadi, P. Shah, O.W. Lee, A. Wang, A. McIver, H. Zheng, X. Wang, X. Xu, A. Jadhav, A. Simeonov, M. Shen, M.B. Boxer, M.D. Hall, Assessing inhibitors of mutant isocitrate dehydrogenase using a suite of pre-clinical discovery assays, *Sci. Rep.* 7 (2017) 12758.
- [15] R. Stupp, W.P. Mason, M.J. van den Bent, M. Weller, B. Fisher, M.J. Taphoorn, K. Belanger, A.A. Brandes, C. Marosi, U. Bogdahn, J. Curschmann, R.C. Janzer, S. K. Ludwin, T. Gorlia, A. Allgeier, D. Lacombe, J.G. Cairncross, E. Eisenhauer, R. O. Mirmanoff, R. European Organisation for, T. Treatment of Cancer Brain, G. Radiotherapy, G. National Cancer Institute of Canada Clinical Trials, Radiotherapy plus concomitant and adjuvant temozolomide for glioblastoma, *N. Engl. J. Med.* 352 (2005) 987–996.
- [16] H.A. Luchman, O.D. Stechishin, N.H. Dang, M.D. Blough, C. Chesnelong, J.J. Kelly, S.A. Nguyen, J.A. Chan, A.M. Weljie, J.G. Cairncross, S. Weiss, An *in vivo* patient-derived model of endogenous IDH1-mutant glioma, *Neuro. Oncol.* 14 (2012) 184–191.
- [17] X. Zhao, Y.J. Zhao, Q. Lin, L. Yu, Z. Liu, H. Lindsay, M. Kogiso, P. Rao, X.N. Li, X. Lu, Cytogenetic landscape of paired neurospheres and traditional monolayer cultures in pediatric malignant brain tumors, *Neuro. Oncol.* 17 (2015) 965–977.
- [18] M. Kogiso, L. Qi, F.K. Braun, S.G. Injac, L. Zhang, Y. Du, H. Zhang, F.Y. Lin, S. Zhao, H. Lindsay, J.M. Su, P.A. Baxter, A.M. Adesina, D. Liao, M.G. Qian, S. Berg, J. A. Muscal, X.N. Li, Concurrent inhibition of neurosphere and monolayer cells of pediatric glioblastoma by aurora A inhibitor MLN8237 predicted survival extension in PDX models, *Clin. Cancer Res.* 24 (2018) 2159–2170.
- [19] Z. Liu, X. Zhao, Y. Wang, H. Mao, Y. Huang, M. Kogiso, L. Qi, P.A. Baxter, T.K. Man, A. Adesina, J.M. Su, D. Picard, K.C. Ho, A. Huang, L. Perlaky, C.C. Lau, M. Chintagumpala, X.N. Li, A patient tumor-derived orthotopic xenograft mouse model replicating the group 3 supratentorial primitive neuroectodermal tumor in children, *Neuro. Oncol.* 16 (2014) 787–799.
- [20] Q. Shu, K.K. Wong, J.M. Su, A.M. Adesina, L.T. Yu, Y.T. Tsang, B.C. Antalfy, P. Baxter, L. Perlaky, J. Yang, R.C. Dauser, M. Chintagumpala, S.M. Blaney, C. C. Lau, X.N. Li, Direct orthotopic transplantation of fresh surgical specimen preserves CD133+ tumor cells in clinically relevant mouse models of medulloblastoma and glioma, *Stem Cells* 26 (2008) 1414–1424.
- [21] L. Yu, P.A. Baxter, X. Zhao, Z. Liu, L. Wadhwa, Y. Zhang, J.M. Su, X. Tan, J. Yang, A. Adesina, L. Perlaky, M. Hurwitz, N. Idamakanti, S.R. Police, P.L. Hallenbeck, S. M. Blaney, M. Chintagumpala, R.L. Hurwitz, X.N. Li, A single intravenous injection of oncolytic picornavirus SVV-001 eliminates medulloblastomas in primary tumor-based orthotopic xenograft mouse models, *Neuro. Oncol.* 13 (2010) 14–27.
- [22] Q. Shu, B. Antalfy, J.M. Su, A. Adesina, C.N. Ou, T. Pietsch, S.M. Blaney, C.C. Lau, X.N. Li, Valproic acid prolongs survival time of severe combined immunodeficient mice bearing intracerebellar orthotopic medulloblastoma xenografts, *Clin. Cancer Res.* 12 (2006) 4687–4694.
- [23] L. Huang, S. Garrett Injac, K. Cui, F. Braun, Q. Lin, Y. Du, H. Zhang, M. Kogiso, H. Lindsay, S. Zhao, P. Baxter, A. Adekunle, T.K. Man, H. Zhao, X.N. Li, C.C. Lau, S. T.C. Wong, Systems biology-based drug repositioning identifies digoxin as a potential therapy for groups 3 and 4 medulloblastoma, *Sci. Transl. Med.* 10 (2018).
- [24] Q. Shu, K.K. Wong, J.M. Su, A.M. Adesina, L.T. Yu, Y.T. Tsang, B.C. Antalfy, P. Baxter, L. Perlaky, J. Yang, R.C. Dauser, M. Chintagumpala, S.M. Blaney, C. C. Lau, X.N. Li, Direct orthotopic transplantation of fresh surgical specimen preserves CD133+ tumor cells in clinically relevant mouse models of medulloblastoma and glioma, *Stem Cells* 26 (2008) 1414–1424.
- [25] L. Yu, P.A. Baxter, H. Voicu, S. Gurusiddappa, Y. Zhao, A. Adesina, T.K. Man, Q. Shu, Y.J. Zhang, X.M. Zhao, J.M. Su, L. Perlaky, R. Dauser, M. Chintagumpala, C.C. Lau, S.M. Blaney, P.H. Rao, H.C. Leung, X.N. Li, A clinically relevant orthotopic xenograft model of ependymoma that maintains the genomic signature of the primary tumor and preserves cancer stem cells *in vivo*, *Neuro. Oncol.* 12 (2010) 580–594.
- [26] T.H. Wang, Y.S. Lin, Y. Chen, C.T. Yeh, Y.L. Huang, T.H. Hsieh, T.M. Shieh, C. Hsueh, T.C. Chen, Long non-coding RNA AOC4P suppresses hepatocellular carcinoma metastasis by enhancing vimentin degradation and inhibiting epithelial-mesenchymal transition, *Oncotarget* 6 (2015) 23342–23357.
- [27] R. Vrtakou, A. Mai, E. Mattila, N. De Franceschi, S.Y. Imanishi, G. Corthals, R. Kuitonen, M. Saari, F. Cheng, E. Torvaldsen, V.M. Kosma, A. Mannermaa, G. Muharram, C. Gilles, J. Eriksson, Y. Soini, J.B. Lorens, J. Ivaska, Vimentin-ERK signaling uncouples slug gene regulatory function, *Cancer Res.* 75 (2015) 2349–2362.
- [28] M. Kogiso, L. Qi, H. Lindsay, Y. Huang, X. Zhao, Z. Liu, F.K. Braun, Y. Du, H. Zhang, G. Bae, S. Zhao, S.G. Injac, M. Sobieski, D. Brunell, V. Mehta, D. Tran, J. Murray, P. A. Baxter, X.J. Yuan, J.M. Su, A. Adesina, L. Perlaky, M. Chintagumpala, D. W. Parsons, C.C. Lau, C.C. Stephan, X. Lu, X.N. Li, Xenotransplantation of pediatric low grade gliomas confirms the enrichment of BRAF V600E mutation and preservation of CDKN2A deletion in a novel orthotopic xenograft mouse model of progressive pleomorphic xanthoastrocytoma, *Oncotarget* 8 (2017) 87455–87471.
- [29] Z. Liu, Y. Yao, M. Kogiso, B. Zheng, L. Deng, J.J. Qiu, S. Dong, H. Lv, J.M. Gallo, X. N. Li, Y. Song, Inhibition of cancer-associated mutant isocitrate dehydrogenases: synthesis, structure-activity relationship, and selective antitumor activity, *J. Med. Chem.* 57 (2014) 8307–8318.
- [30] M. Sasaki, C.B. Knobbe, J.C. Munger, E.F. Lind, D. Brenner, A. Brustle, I.S. Harris, R. Holmes, A. Wakeham, J. Haight, A. You-Ten, W.Y. Li, S. Schalm, S.M. Su, C. Vitanen, G. Reifenberger, P.S. Ohashi, D.L. Barber, M.E. Figueroa, A. Melnick, J.C. Zuniga-Pflucker, T.W. Mak, IDH1 (R132H) mutation increases murine haematopoietic progenitors and alters epigenetics, *Nature* 488 (2012) 656–659.
- [31] Y. Zhou, L. Yang, X. Zhang, R. Chen, X. Chen, W. Tang, M. Zhang, Identification of potential biomarkers in glioblastoma through bioinformatic analysis and evaluating their prognostic value, *Biomed. Res. Int.* 2019 (2019), 6581576.
- [32] Y. Matsuda, T. Ishiwata, H. Yoshimura, M. Hagio, T. Arai, Inhibition of nestin suppresses stem cell phenotype of glioblastomas through the alteration of post-translational modification of heat shock protein HSPA8/HSC71, *Cancer Lett.* 357 (2015) 602–611.
- [33] A. Lai, S. Kharbanda, W.B. Pope, A. Tran, O.E. Solis, F. Peale, W.F. Forrest, K. Pujara, J.A. Carrillo, A. Pandita, B.M. Ellingson, C.W. Bowers, R.H. Soriano, N. O. Schmidt, S. Mohan, W.H. Yong, S. Seshagiri, Z. Modrusan, Z. Jiang, K.D. Aldape, P.S. Mischel, L.M. Liaw, C.J. Escovedo, W. Chen, P.L. Nghiemphu, C.D. James, M. D. Prados, M. Westphal, K. Lamszus, T. Cloughesy, H.S. Phillips, Evidence for

- sequenced molecular evolution of IDH1 mutant glioblastoma from a distinct cell of origin, *J. Clin. Oncol.* 29 (2011) 4482–4490.
- [34] S. Nobusawa, T. Watanabe, P. Kleihues, H. Ohgaki, IDH1 mutations as molecular signature and predictive factor of secondary glioblastomas, *Clin. Cancer Res.* 15 (2009) 6002–6007.
- [35] E. Cuyas, S. Fernandez-Arroyo, B. Corominas-Faja, E. Rodriguez-Gallego, J. Bosch-Barrera, B. Martin-Castillo, R. De Llorens, J. Joven, J.A. Menendez, Oncometabolic mutation IDH1 R132H confers a metformin-hypersensitive phenotype, *Oncotarget* 6 (2015) 12279–12296.
- [36] S.E. Combs, S. Rieken, W. Wick, A. Abdollahi, A. von Deimling, J. Debus, C. Hartmann, Prognostic significance of IDH-1 and MGMT in patients with glioblastoma: one step forward, and one step back? *Radiat. Oncol.* 6 (2011) 115.
- [37] S. Li, A.P. Chou, W. Chen, R. Chen, Y. Deng, H.S. Phillips, J. Selfridge, M. Zurayk, J. Lou, R.G. Everson, K.C. Wu, K.F. Faull, T. Cloughesy, L.M. Liau, A. Lai, Overexpression of isocitrate dehydrogenase mutant proteins renders glioma cells more sensitive to radiation, *Neuro Oncol.* 15 (2013) 57–68.
- [38] T.Q. Tran, X.H. Lowman, M. Kong, Molecular pathways: metabolic control of histone methylation and gene expression in cancer, *Clin. Cancer Res.* 23 (2017) 4004–4009.
- [39] C. Diquigiovanni, C. Bergamini, C. Evangelisti, F. Isidori, A. Vettori, N. Tiso, F. Argenton, A. Costanzini, L. Iommarini, H. Anbunathan, U. Pagotto, A. Repaci, G. Babbi, R. Casadio, G. Lenaz, K.J. Rhoden, A.M. Porcelli, R. Fato, A. Bowcock, M. Seri, G. Romeo, E. Bonora, Mutant MYO1F alters the mitochondrial network and induces tumor proliferation in thyroid cancer, *Int. J. Cancer* 143 (2018) 1706–1719.
- [40] D.M. Gay, R.A. Ridgway, M. Muller, M.C. Hodder, A. Hedley, W. Clark, J.D. Leach, R. Jackstadt, C. Nixon, D.J. Huels, A.D. Campbell, T.G. Bird, O.J. Sansom, Loss of BCL9/9l suppresses Wnt driven tumourigenesis in models that recapitulate human cancer, *Nat. Commun.* 10 (2019) 723.
- [41] Y.M. Luo, N.X. Xia, L. Yang, Z. Li, H. Yang, H.J. Yu, Y. Liu, H. Lei, F.X. Zhou, C. H. Xie, Y.F. Zhou, CTC1 increases the radioresistance of human melanoma cells by inhibiting telomere shortening and apoptosis, *Int. J. Mol. Med.* 33 (2014) 1484–1490.
- [42] E.M. Goellner, B. Grimme, A.R. Brown, Y.C. Lin, X.H. Wang, K.F. Sugrue, L. Mitchell, R.N. Trivedi, J.B. Tang, R.W. Sobol, Overcoming temozolomide resistance in glioblastoma via dual inhibition of NAD⁺ biosynthesis and base excision repair, *Cancer Res.* 71 (2011) 2308–2317.
- [43] T.C. Chen, D.R. Hinton, R. Zidovetzki, F.M. Hofman, Up-regulation of the cAMP/PKA pathway inhibits proliferation, induces differentiation, and leads to apoptosis in malignant gliomas, *Lab. Invest.* 78 (1998) 165–174.
- [44] L. Frattola, N. Canal, C. Ferrarese, C. Tonini, G. Tonon, R. Villani, M. Trabucchi, Multiple forms of protein kinase from normal human brain and glioblastoma, *Cancer Res.* 43 (1983) 1321–1324.
- [45] E. Kirches, G. Krause, M. Warich-Kirches, S. Weis, T. Schneider, B. Meyer-Puttlitz, C. Mawrin, K. Dietzmann, High frequency of mitochondrial DNA mutations in glioblastoma multiforme identified by direct sequence comparison to blood samples, *Int. J. Cancer* 93 (2001) 534–538.
- [46] G. Marucci, A. Maresca, L. Caporali, A. Farnedi, C.M. Betts, L. Morandi, D. de Biase, S. Cerasoli, M.P. Foschini, E. Bonora, M. Vidone, G. Romeo, E. Perli, C. Giordano, G. d'Amati, G. Gasparre, A. Baruzzi, V. Carelli, V. Eusebi, Oncocytic glioblastoma: a glioblastoma showing oncocytic changes and increased mitochondrial DNA copy number, *Hum. Pathol.* 44 (2013) 1867–1876.
- [47] E. Reznik, M.L. Miller, Y. Senbabaoglu, N. Riaz, J. Sarungbam, S.K. Tickoo, H.A. Al-Ahmadie, W. Lee, V.E. Seshan, A.A. Hakimi, C. Sander, Mitochondrial DNA copy number variation across human cancers, *Elife* 5 (2016).
- [48] V. Dmitrenko, K. Shostak, O. Boyko, O. Khomenko, V. Rozumenko, T. Malisheva, M. Shamayev, Y. Zozulya, V. Kavsan, Reduction of the transcription level of the mitochondrial genome in human glioblastoma, *Cancer Lett.* 218 (2005) 99–107.
- [49] A. Dickinson, K.Y. Yeung, J. Donoghue, M.J. Baker, R.D. Kelly, M. McKenzie, T. G. Johns, J.C. St John, The regulation of mitochondrial DNA copy number in glioblastoma cells, *Cell Death Differ.* 20 (2013) 1644–1653.